Atmospheric
Chemistry
and Physics
Discussions

Open Access

How important are cyclones for emitting mineral dust aerosol in North Africa?

S. Fiedler[1], K. Schepanski[2], P. Knippertz[1,*], B. Heinold[2], and I. Tegen[2]

[1]School of Earth and Environment, University of Leeds, LS2 9JT Leeds, UK
[2]Leibniz Institute for Tropospheric Research (TROPOS), Permoser Str. 15, 04318 Leipzig, Germany
[*]now at: Karlsruher Institute of Technology, Kaiserstr. 12, 76131 Karlsruhe, Germany

Correspondence to: S. Fiedler (eesfi@leeds.ac.uk)

Discussion Paper | Discussion Paper | Discussion Paper | Discussion Paper

ACPD

13, 32483–32528, 2013

Dust emission by cyclones

S. Fiedler et al.

Title Page

Abstract	Introduction
Conclusions	References
Tables	Figures

|◀ | ▶|

◀ | ▶

Back | Close

Full Screen / Esc

Printer-friendly Version

Interactive Discussion

Abstract

This study presents the first quantitative estimate of the mineral dust emission associated to atmospheric depressions and migrating, long-lived cyclones in North Africa. Results from a tracking algorithm are combined with dust emission flux calculations based on ERA-Interim data from the European Centre for Medium-Range Weather Forecasts for 1989–2008. The results highlight that depressions are abundant and associated with 55 % of the dust emission amount annually and spatially averaged over North African dust sources. Even larger contributions to dust emission from depressions are found south of the Atlas Mountains during spring with regionally up to 90 %. It is spring when the largest monthly totals of 250–380 $\mathrm{g\,m^{-2}}$ of dust emission occur in North Africa. The remaining months have a total dust emission smaller than 80 $\mathrm{g\,m^{-2}}$. In summer, depressions, particularly Saharan heat lows, coincide with up to 90 % of the seasonal total dust emission over wide areas of North Africa.

In contrast to depressions, migrating cyclones that live for more than two days are rare and are associated to 4 % of the annual and spatial dust emission average. Migrating cyclones over North Africa occur primarily in spring north of 20° N with eastwards trajectories and typical life times of three to seven days. Regionally larger seasonal totals of dust emission are associated to cyclones with up to 25 % over Libya. In summer, near-surface signatures of African Easterly Waves (AEWs) emit regionally up to 15 % of the total emission. The diurnal cycle of dust emission underlines that emission associated to cyclones at mid-day is substantially larger than at night by a factor of three to five. Soil moisture weakens dust emission during cyclone passage by 10 %. Despite the overall small contribution of migrating cyclones to dust emission, cyclones coincide with particularly intense dust emission events exceeding the climatological mean flux by a factor of four to eight. This implies, that both depressions and migrating, long-lived cyclones are important for dust emission in North Africa.

1 Introduction

The accurate simulation of mineral dust aerosol in the Earth system is one of the great challenges of current atmospheric research. Dust aerosol is important due to its proposed but uncertain effects on the radiation transfer in the atmosphere with implications
5 for the water and energy cycle, as well as effects on eco-systems and humans (Carslaw et al., 2010; Shao et al., 2011; Knippertz and Todd, 2012, and references therein). Despite these impacts of dust aerosol, estimates of the annual total of dust emission from state-of-the-art climate models vary from 400 to 2200 Tg for North Africa (Huneeus et al., 2011), the largest dust source on Earth. Further reduction of this modelling un-
10 certainty depends on improving the representation of dust emission. Both the realistic description of soil properties and meteorological mechanisms for peak wind generation are important. The wind speed near the surface is particularly crucial as it controls the onset of dust emission, and the magnitude of the flux non-linearly (e.g. Marticorena and Bergametti, 1995; Tegen et al., 2002).
15   A systematic analysis of mechanisms generating peak winds strong enough for mobilizing dust provides the basis for evaluating dust emission from atmospheric models. Recently a number of studies have addressed meteorological processes for dust emission with a clear focus on the meso-scale. Cold pool outflows from convective downdrafts (haboobs) are suggested as an important dust storm type in summertime West
20 Africa (Marsham et al., 2011; Heinold et al., 2013). A 40 day horizontally high-resolved simulation suggests that haboobs generate about half of the dust aerosol amount in this region, but a physical parameterization for atmospheric models with coarse spatial resolution is currently missing (Heinold et al., 2013). Another important process for dust emission is the nocturnal low-level jet (NLLJ), which frequently forms in North Africa
25 (Schepanski et al., 2009; Fiedler et al., 2013). Based on a 32-yr climatology, up to 60 % of the dust emission is associated to NLLJs in specific regions and seasons (Fiedler et al., 2013).

Dust emission by cyclones

S. Fiedler et al.

The main meteorological driver for the largest dust emission amount of the continent that occurs north of 20° N between December and May (Fiedler et al., 2013), however, is not well quantified. It is this time of year when cyclones affect the region (e.g. Alpert and Ziv, 1989; Winstanley, 1972; Hannachi et al., 2011). The core of these cyclones can either lie over the continent itself or further north in the Mediterranean region (e.g. Maheras et al., 2001; Schepanski and Knippertz, 2011). Several studies suggest that cyclones can cause dust storms (Bou Karam et al., 2010; Hannachi et al., 2011; Schepanski et al., 2009; Schepanski and Knippertz, 2011), although a case study by Knippertz and Fink (2006) for the exceptionally strong and continental-scale dust storm in March 2004 gives evidence that a cyclone only produces one part of the associated dust emission. The remaining dust mobilization is linked to strong northeasterly Harmattan winds. These Harmattan surges manifest themselves by an increased horizontal pressure gradient between the post cold frontal ridge and the prevailing low pressure over the continent. Harmattan surges can lead to continental scale dust outbreaks with subsequent transport towards the Sahel, Atlantic Ocean and beyond. Klose et al. (2010) show that about half of dust suspended over the Sahel may be linked to a pressure pattern typical of Harmattan surges: a low over the Arabian Peninsula and the Azores High expanding eastwards into the continent. The mass of dust emission associated to cyclones has not been estimated before. The aim of the present study is to reveal how much dust emission is linked to migrating cyclones affecting North Africa.

Previous work on cyclones influencing North Africa focus on the meteorological analysis in the Mediterranean basin. Alpert et al. (1990) use five years of analysis data from the European Centre for Medium-Range Weather Forecasts (ECMWF) for analysing Mediterranean cyclones statistically. A longer time period of 18 yr of ECMWF re-analysis is exploited by Trigo et al. (1999) for cyclone tracking. The contributing factors of cyclogenesis in the Mediterranean region is investigated later by Trigo et al. (2002). Maheras et al. (2001) present a 40-yr climatology of surface cyclones based on re-analysis from the National Centers for Environmental Prediction (NCEP) and underline the variability of both the position and the core pressure of cyclones with the

time of day. Since the method does not have a criterion for cyclone migration, the climatology by Maheras et al. (2001) includes heat lows and orographic depressions. NCEP data is also used for a springtime climatology of cyclones north of 20° N for 1958–2006 (Hannachi et al., 2011). Hodges et al. (2011) compares cyclone climatologies derived from state-of-the-art re-analysis showing spatial differences of track densities and cyclone intensity. All of these studies highlight distinct regions that are prone to frequent cyclogenesis. These are over sea the Aegean Sea, the Gulf of Genoa and the Black Sea (Trigo et al., 2002). Regions of frequent cyclogenesis in northern Africa lie to the south of the Atlas Mountains, and east of the Hoggar Mountains (Alpert and Ziv, 1989; Trigo et al., 1999; Maheras et al., 2001; Schepanski and Knippertz, 2011; Winstanley, 1972). Cyclones may further form or intensify over Libya, also termed Sharav or Khamsin cyclones (Alpert and Ziv, 1989, e.g.) which are thought to be the main driver for dust transport towards the Eastern Mediterranean (Moulin et al., 1998; Winstanley, 1972). Classically the term "Sharav" is used for heat waves in Israel, for which cyclones from Africa are one of the meteorological conditions (Winstanley, 1972). Most of the cyclones in the Mediterranean basin form between December and May, when the temperature contrast between land and sea is largest.

Cyclogenesis in Northwest Africa occurs east of an upper level trough where positive vorticity advection supports the formation of a depression near the surface. These troughs advect cool air masses at their western side towards the Sahara and transport Saharan air northwards at their eastern side (e.g. Maheras et al., 2001; Knippertz and Fink, 2006). The interaction with orography can lead to cyclogenesis at the lee side of mountain ranges. In North Africa, the position of lee cyclogenesis is typically the southern side of the Atlas Mountains (e.g. Schepanski and Knippertz, 2011; Trigo et al., 2002). Migrating lee cyclones usually follow east- to northeastward trajectories with propagation speeds around $10\,\mathrm{m\,s^{-1}}$ (e.g. Alpert and Ziv, 1989; Alpert et al., 1990; Bou Karam et al., 2010; Hannachi et al., 2011). They can advect hot, dry and dusty air towards the Eastern Mediterranean, but may also bring rainfall (Winstanley, 1972) with flood risk in Israel (Kahana et al., 2002). Unusually deep cyclones over the Western

Mediterranean that move from Algeria northwards are documented for winter that can cause high impact weather (Homar et al., 2002, 2007; Homar and Stensrud, 2004).

In contrast to cyclones at the northern fringes of the continent, low latitudes are characterized by shallow depressions. Depressions in form of heat lows build in response to strong solar irradiation, the location of which changes in the course of year. In North Africa the heat low moves from positions near the equator in the east between November and March towards West Africa between April and October (Lavaysse et al., 2009). The Saharan heat low during summer is typically quasi-stationary over several days to weeks (Todd et al., 2013) and coincides with high concentrations of dust aerosol (e.g. Knippertz and Todd, 2010).

A migrating depression type originating in low-latitudes is the Sudano-Saharan depression the concept of which is described in classical literature and has recently been revised (Schepanski and Knippertz, 2011, and references therein). These depressions form in the central Sahara, usually southwest of the Tibesti Mountain. They initially migrate westwards before turning anticyclonicly over West Africa to track eastwards over northern parts of the continent. Analysis of 20 yr of ECMWF ERA-Interim re-analysis suggests that Sudano-Saharan depressions are rare and too shallow for causing sufficiently high wind speeds for significant amounts of dust uplift (Schepanski and Knippertz, 2011).

Other migrating depressions at low latitudes are surface signatures of African Easterly Waves (AEW). Based on upper-air soundings, Burpee (1972) shows that AEWs form south of the African Easterly Jet (AEJ) at 700 hPa along 10° N. The AEJ results from the horizontal temperature contrast between the hot Saharan air poleward and the cooler air masses equatorward of the AEJ. Burpee (1972) suggests that the wind shear at the AEJ is the origin of wave-like disturbances. More recent works suggest deep convection as a trigger of AEWs (e.g. Mekonnen et al., 2006; Thorncroft et al., 2008). The main genesis region of AEWs remains controversial and ranges from 10° E to 40° E (Burpee, 1972; Mekonnen et al., 2006; Thorncroft and Hodges, 2000; Thorncroft et al., 2008, and references therein) from where they propagate westwards with

the mean flow. AEWs occur about every three to five days between June and September with a peak activity at the beginning of August (Burpee, 1972; Jones et al., 2003). At 850 hPa, AEW signatures occur both north and south of the AEJ axis at 10° N and 20° N (Mekonnen et al., 2006). AEW signatures at 850 hPa are most frequently found
5 in West Africa with up to six events between May and October around 20° N and 10° W (Thorncroft and Hodges, 2000). AEWs are linked to variability of dust mobilization and concentration over West Africa although the diurnal cycle seems similarly important (Luo et al., 2004). Knippertz and Todd (2010) argue that dust emission associated to AEWs is driven by embedded haboobs and NLLJs. Predominant emission in the late af-
10 ternoon and evening is an indication for haboobs (Marsham et al., 2011; Heinold et al., 2013) while morning emissions can be linked to the breakdown of NLLJs (Schepanski et al., 2009; Fiedler et al., 2013). AEWs are also important for atmospheric transport of dust aerosol (Jones et al., 2003) and are linked to tropical cyclone formation (Hopsch et al., 2007).
15 Horizontal pressure gradients during the presence of depressions can be large enough for generating dust storms (Winstanley, 1972; Hannachi et al., 2011). In addition to wind speed, the presence of soil moisture can have important implications for dust emission (Fecan et al., 1999). An increase of soil moisture strengthens the bonding forces between soil particles constraining higher wind speeds for dust emis-
20 sion (Cornelis and Gabriels, 2003; Fecan et al., 1999). While precipitation amounts and therefore soil moisture are generally small in wide areas across the Sahara, cyclones are an important source for rainfall in North Africa (Hannachi et al., 2011) and may be able to moisten the soil sufficiently for increasing the threshold of dust emission onset. This soil moisture effect is predominantly expected for cyclones along the North African
25 coast between December and May, and near-surface signatures of AEWs at the southern fringes of the Sahara desert between May and September. The magnitude of the soil moisture effect during cyclone passage is, however, not well quantified.

The present study is the first climatological estimate of the mass of emitted dust aerosol associated to depressions and migrating, long-lived cyclones in North Africa.

Dust emission by cyclones

S. Fiedler et al.

Depressions are defined as minima in the geopotential height at 925 hPa that are identified and tracked with an automatic algorithm. Minima in the field of geopotential height are termed cyclones if they migrate, live for more than two days, and have a decreasing core pressure at the beginning of their life cycle. The depression and cyclone tracks are combined with dust emission calculations driven by ECMWF ERA-Interim data. Details of the method are explained in Sect. 2. Section 3 presents the results for the climatology of depressions and cyclones for dust emission. Conclusions are drawn in Sect. 4.

2 Method

2.1 Depression and cyclone identification

The present study uses the depression tracks over North Africa for 1989–2008 retrieved by Schepanski and Knippertz (2011). Schepanski and Knippertz (2011) investigate Sudano-Saharan depressions by using the tracking algorithm from Wernli and Schwierz (2006) with modifications for low latitudes. Threshold values are adapted and the original input fields of mean sea level pressure are replaced by the geopotential height at 925 hPa that represent North African conditions better. The automated algorithm determines minima relative to the adjacent grid cells and is applied to the ERA-Interim re-analysis with a horizontal resolution of 1° (Dee et al., 2011). Even though the input data set is six-hourly, minima are identified daily at 00:00 UTC in order to avoid miss-tracking caused by the large diurnal cycle of the geopotential height at low levels over North Africa (Schepanski and Knippertz, 2011). The influence of the time of day on a depression identification is shown by Maheras et al. (2001).

Once a minimum is identified, the corresponding area of the depression is determined by the closed contour that lies furthest away from the centre. The value of the contour interval is 4 gpm corresponding to about 0.5 hPa (Schepanski and Knippertz, 2011). Depressions are connected to a track if two consecutive positions lie within

1000 km. This criterion allows a maximum speed of $11.6\,\mathrm{m\,s^{-1}}$ that is sufficient for North Africa (Schepanski and Knippertz, 2011).

The criteria from Schepanski and Knippertz (2011) used to filter tracks of Sudano-Saharan depressions are not applied here. Instead, a broader investigation of depressions and migrating cyclones over North Africa is intended. Depressions are all identified minima in the geopotential height at 925 hPa. The selection of migrating cyclones from the original set of depressions requires generalized criteria applicable for the entire domain and time period. Note that migrating cyclones include both near-surface signatures of AEWs and cyclones. Both are termed cyclones in this paper and identified by the following filter:

1. Cyclones have to be identified in at least three consecutive nights reflecting a life time of 48 h as the minimum time period for a complete life cycle of a cyclone. This assumption complies with life times given in the literature (Hannachi et al., 2011; Bou Karam et al., 2010).

2. Each cyclone has to propagate over a pre-defined horizontal distance between genesis and lysis. The mean propagation speed is defined as the maximum displacement during the life time of the system calculated from the range of longitudes and latitudes of centre positions. The threshold for the propagation speed is 5° per day corresponding to a mean cyclone speed of 5–$6\,\mathrm{m\,s^{-1}}$. This generous criterion is well below migration speeds reported for cyclones over North Africa (Alpert and Ziv, 1989; Bou Karam et al., 2010; Knippertz and Todd, 2010; Schepanski and Knippertz, 2011).

3. The propagation speed alone does not successfully exclude all identified cases of the Saharan heat low, the mean position of which migrates over time. In order to exclude most heat lows, the identified cyclones have to have a decreasing core pressure between the first and second night. This criterion reflects cyclogenesis and successfully reduces the number of identified cyclones in summertime West Africa. Tracks of filling cyclones in the Mediterranean region are also excluded by

this criterion, particularly frequent in the east during spring. Sensitivity tests show that reducing the number of cyclones in the Mediterranean basin has a negligible effect on the contribution to dust emission (Sect. 3.5). This suggests that filling cyclones with centres away from dust sources do not generate wind speeds suf-
⁵ ficiently large for mobilizing dust.

2.2 Dust emission

Mineral dust emission is calculated for 1989–2008 with the dust emission model by Tegen et al. (2002) following the experiment setup in Fiedler et al. (2013). The dust model is driven by three-hourly 10 m-wind speeds and soil moisture of the uppermost
¹⁰ soil layer from ERA-Interim forecasts (Dee et al., 2011). These forecasts are for 12 h initialized at 00:00 and 12:00 UTC, and interpolated onto a horizontal grid of 1°. ERA-Interim re-analysis produces the best diurnal cycle of wind speed amongst state-of-the-art re-analysis projects compared to flux tower observations over land (Decker et al., 2012). Choosing ERA-Interim forecasts is motivated by the higher temporal resolution
¹⁵ compared to the six-hourly re-analysis product that is not sufficient for resolving all wind speed maxima during the day (Fiedler et al., 2013). Statistics of the near-surface wind speed from these short-term forecasts are found to be close to the six-hourly re-analysis of ERA-Interim (Fiedler et al., 2013).

Preferential dust sources are prescribed using the dust source activation frequency
²⁰ map derived from satellite observations (Schepanski et al., 2007, 2009). A source is defined as a region where at least two dust emission events are detected between March 2006 and February 2008 as in Fiedler et al. (2013). Depending on surface properties like vegetation fraction, soil moisture, and roughness length, dust emission occurs in these sources when the particle-size dependent threshold of the 10 m-wind
²⁵ speed is exceeded (for details see Marticorena and Bergametti, 1995; Tegen et al., 2002). Soil moisture has to be below $0.28\,\mathrm{m^3\,m^{-3}}$, the field capacity assumed for silt and clay soil types. An experiment without soil moisture is run for estimating the effect of water in the topsoil on dust emission.

Calculating the contribution of depressions and cyclones to dust emission requires the definition of an area affected by associated peak winds. The tracking algorithm determines an area for the grid boxes lying within the outermost closed contour of the geopotential height at 925 hPa at mid-night. This centre area is used for analysing the track density per season (Sect. 3.1 and 3.2). Dust emission, however, may occur in an area larger than the centre, e.g. near the cold front. In order to include these dust emissions in the climatology, a cyclone-affected area is approximated by a circle around the identified minimum in the geopotential height. This area is calculated at mid-night and used for selecting the three-hourly dust emission associated to the depression or cyclone between 15:00 UTC of the previous day and 12:00 UTC of the same day (Sect. 3.4 and 3.5). The radius of this circle is set to 10°, a value corresponding to a latitudinal distance of 964 km at 30° N. The choice of 10° is justified by previous studies (e.g. Bou Karam et al., 2010) and tested by sensitivity experiments. These show that even when the radius of the circle is doubled, the spatial pattern of the fraction of dust emission associated to cyclones shown in Sect. 3.5 is robust.

Figure 1 shows the cyclone-affected area and false colour images derived from thermal and infrared radiation measurements from the "Spinning Enhanced Visible and Infrared Imager" (SEVIRI) of the geostationary Meteosat Second Generation (MSG) satellite (e.g. Schepanski et al., 2007, 2009). The typical horizontal extent of these cyclones, visible by the curling cloud band (red) and indicated by a circle around the cyclone centre, is on the order of 10°. Dust aerosol is visible near the cloud band, but parts of it is likely obscured by clouds. At 9 March 2013, dust emission also occurs over southern West Africa (Fig. 1b), highlighted by an ellipse. These emissions are not directly related to the cyclone but likely caused by a Harmattan surge associated with the post frontal ridge (e.g. Knippertz and Fink, 2006).

3 Results

3.1 Climatology of depressions

Figure 2 shows the seasonal mean track density of depressions identified by the algorithm. During winter, depressions are found over the Mediterranean basin with 40–100 events in the 20-yr period (Fig. 2a), i.e. 2–5 cyclones per winter. Hot spots of similarly large track densities lie to the south of the High Atlas and to the west of the Ethiopian Highlands (refer to Fig. 5 for geographical terms). The origin of these depressions may be partly related to lee troughs that are associated with closed contours in the geopotential height at 925 hPa. In the case of the Ethiopian Highlands, the heat low that is located here during winter (Lavaysse et al., 2009) may explain another large portion of identified depressions. The general location of depressions over the Mediterranean Sea and the lee hot spot of the Atlas Mountains are in agreement with previous studies (Trigo et al., 1999; Maheras et al., 2001). The exact number and location of hot spots, however, depend on the underlying data set and identification technique (e.g. Maheras et al., 2001; Hannachi et al., 2011; Hodges et al., 2011, and references therein).

Depressions in spring are more frequent than in winter with 10–100 depressions over most areas (Fig. 2b). The hot spot south of the High Atlas dominates the climatology in the north with depression numbers around 200, i.e. ten depressions per season. A secondary maximum can be identified at the northern side of the Hoggar Mountains with up to 100 depressions. These two hot spots agree with the formation of springtime cyclones from the literature, although the exact locations and frequencies differ (Maheras et al., 2001; Hannachi et al., 2011). Other studies for springtime North Africa find a single hot spot for depressions (Trigo et al., 1999). Reasons for these differences are the choice of a different data basis, time period, identification method, as well as the time of day due to the influence of daytime heating on heat lows (Maheras et al., 2001). Further hot spots that can be related to lee troughs are found southwest of all mountains in the central Sahara due to the prevailing northeasterly Harmattan winds during this season. Maxima in the vicinity of the Ethiopian Highlands and the Ennedi

Mountains reach around 100 depressions. Wide areas in the centre of North Africa have track densities around 20 depressions. The similarity to the location of the heat low climatology by Lavaysse et al. (2009) suggests that these depressions are heat lows.

5   Between June and August, West Africa has track densities of 40–200 depressions (Fig. 2c). Here, the Saharan heat low dominates the climatology while AEWs regularly influence the meteorological conditions (Lavaysse et al., 2009; Thorncroft and Hodges, 2000; Luo et al., 2004). Similar track densities are found in the vicinity of mountains where the Saharan heat low influences the occurrence of depressions, predominantly
10 at the Hoggar Massif (Lavaysse et al., 2009). The heat low over West Africa and the hot spots near mountains in the central Sahara are present in summer and autumn but the relative importance changes (Fig. 2d). In autumn, the track density west of the Ethiopian Highlands is larger with values around 200 depressions, while the track densities over West Africa decrease to less than 100 depressions. This pattern is coherent
15 with the shift of the heat low from West Africa towards the southeast near the equator (Lavaysse et al., 2009). Heat lows and depressions in the vicinity of mountains seem to dominate the climatology of depressions throughout the year. Migrating cyclones and surface signatures of AEWs are separately investigated in the following section.

3.2   Climatology of cyclones

20 Migrating cyclones and surface signatures of AEWs are filtered as described in Sect. 2.1. The term cyclone is used for both types in the following. Cyclones regularly form over North Africa and the Mediterranean region, but the number of events is substantially smaller than the number of depressions. In the annual mean, ten cyclones occur in the sub-domain investigated, namely 0° to 40° N and 20° W to 45° E.
25 Figure 3a shows the seasonal fraction of the total number of 196 cyclones that pass the filter. The analysis reveals that most of the cyclones form between March and May with 37 %. The remaining seasons have fewer events with roughly 20 % each.

Dust emission by cyclones

S. Fiedler et al.

Title Page

Abstract | Introduction

Conclusions | References

Tables | Figures

◄ | ►I

◄ | ►

Back | Close

Full Screen / Esc

Printer-friendly Version

Interactive Discussion

The time series of the total number of cyclones per year is shown in Fig. 3b. The year-to-year variability of cyclone activity is relatively large with a factor three to four. The years with most identified events are 2003 with 19 cyclones, followed by 2002 with 16, 1996 and 1999 with 14 events each. The most inactive years are 1998, 2000, 2001 and 2007 with five to seven cyclones each. Most of this variability can be explained by the cyclone activity during spring. The year-to-year variability for this season is particularly large. Years with a large event number experience 6–12 cyclones, while years with low activity have one to three events between March and May.

Figure 4 shows the spatial distribution of cyclone centres per season in the 20-yr period. The dominant cyclone track between December and February stretches from the Aegean Sea to Cyprus (Fig. 4a). Some areas in this track count at least ten cyclones in the period, i.e. one cyclone every second year. Including filling cyclones doubles the number of cyclones passing the eastern Mediterranean. Few cyclones are situated over the African continent during winter. Maxima around six cyclones are limited to areas along the northern coast between Tunis, Tunisia, and Tobruk, Libya. Similarly large values are found north of the Great Eastern Erg and the south-eastern side of the Tell Atlas, Algeria and Tunisia. Up to six cyclones track north of the Hoggar Mountains, Algeria, south of the High Atlas Range, Morocco, and south of Tripoli, Libya.

Between March and May, cyclones occur most frequently over North Africa (Fig. 4b). Cyclones at the southern side of the High Atlas are identified up to eight times between 1989 and 2008. Up to ten cyclones track over areas of the Great Eastern Erg between the Tell Atlas Mountains and the Hoggar Massif, Tunisia and Algeria. This cyclone frequency is comparable to the cyclone track in the wintertime Mediterranean Sea (Fig. 4a and b). The eastern side of the Al-Hamra Plateau, Libya, also shows around ten cyclones which is consistent with the reported ideal conditions in this region (Alpert et al., 1990; Pedgley, 1972).

The peak cyclone activity north of 25° N in winter and spring rapidly decreases as the year progresses. Cyclones are rare in summer with maxima of two cyclones (Fig. 4c). Maxima of the track density are shifted southward to West Africa with six to ten events

along 20° N. Here, the cyclones are connected to AEWs that are strong enough to form a signature near the surface. It is interesting that the track density peaks in the lee of mountains similar to the springtime maximum in the north. These hot spots are situated at the western sides of the mountains Tibesti, Aïr, and Adrar des Iforas. The peak at the Tibesti is particularly strong with 8–10 cyclones. The location suggests that the interaction of the flow with mountains aid the deepening and formation of closed contours in the geopotential height at 925 hPa. A much larger area of maximum track densities of 5–10 is found over Mali and Mauritania centred around 20° N, a region known for frequent occurrence of AEW signatures at higher altitudes (Thorncroft and Hodges, 2000; Mekonnen et al., 2006). The spatial pattern of cyclone tracks is similar in autumn, but the absolute number is smallest (Fig. 4d). The regions of most frequent cyclone occurrence are summarized in Fig. 5. These are the northern fringes of North Africa between December and May and West Africa from June to August. The characteristics of the cyclones are investigated in the following.

3.3 Characteristics of cyclones

Figure 6 shows the life time and zonal displacement of the identified cyclones for areas north and south of 20° N over the continent. In the north, cyclogenesis occurs 56 times during the 20-yr period, more than half of which form between March and May (32 cyclones). Most of these cyclones have their origin in the vicinity of the Atlas Mountains with 26 cyclones between 15° W and 10° E. Cyclones in the north frequently live for three days in spring (Fig. 6a). Life times between five and seven days are similarly common for the season. Springtime cyclones predominantly follow eastward tracks in the north (Fig. 6c). The migration distance is most often 30° to the east, closely followed by 20° and 10°. Some cyclones with eastward trajectories also form south of 20° N during spring (Fig. 6d). Wintertime cyclones have a similar distribution of the migration direction. The prevailing eastward migration in the north is in agreement with previous studies (e.g. Alpert et al., 1990; Hannachi et al., 2011).

South of 20° N, the seasonality of cyclogenesis is different. Out of 50 cyclones forming here in total, 36 % occur between June and August followed by 26 % and 28 % in autumn and spring, respectively. Figure 6b shows the cyclone life time for the south. Here, the majority of cyclones are identified over three to four days. Summertime cyclones also live frequently for six days. The prevailing migration direction during summer and autumn is westwards by mostly 20–30° (Fig. 6d) that is consistent with the propagation of AEWs (Burpee, 1972; Thorncroft and Hodges, 2000).

3.4 Dust emission associated to depressions

Annually and spatially averaged across dust sources of North Africa, 55 % of the dust emission is associated to depressions. Regionally larger fractions of dust emission coincide with depressions that are shown in Fig. 7. Areas in northern and western Africa have dust emission associated to depressions of up to 80 %. The seasonal distribution of these fractions is shown in Fig. 8. Contributions from depressions to dust emission during winter have values below 50 % in most of North Africa (Fig. 8a). Larger fractions are associated to depressions in West Sahara, Libya, Tunisia, and Sudan with values of up to 80 %. These hot spots coincide with the frequent formation of depressions in the north of the continent and in the lee of the Ethiopian Highlands. Spring shows even larger contributions to dust emission from depressions in wide areas to the north of 25° N and west of 10° E with up to 90 % (Fig. 8b).

Depressions in summer are linked to up to 90 % of the regional dust emission across most of North Africa (Fig. 8c). In autumn, similarly large values for dust emission associated to depressions are found along the northern and western margins of the continent, west of the Hoggar Massif and west of the Ethiopian Highlands (Fig. 8d). The large and widespread contributions from depressions in summer is surprising as other dust-emitting processes have been discussed in the literature (e.g. Fiedler et al., 2013; Heinold et al., 2013). An important mechanism for dust emission in summertime West Africa is the downward mixing of momentum from NLLJs. NLLJs are frequently embedded along the margins of the West African heat low (Fiedler et al., 2013). Estimating

the contribution to dust emission from the heat low includes the emissions associated to NLLJs and possibly other processes occurring within the assumed radius of 10°. The example of the embedded NLLJ illustrates that the results for the dust emission associated to depressions are not necessarily excluding other processes. These contributions to dust emission are expected to change if only migrating and long-lived depressions are taken into account. These systems, termed cyclones in the following, are investigated next.

3.5 Dust emission associated to cyclones

3.5.1 Seasonal climatology

The climatology is shown as absolute emissions associated to migrating cyclones first followed by the presentation of the relative contribution to dust emission. Figure 9 shows the seasonal total of dust emission and the number of intense emission events associated to cyclones averaged over the 20-yr period. Intense emission is defined for fluxes greater than $10^{-5}\,\mathrm{g\,m^{-2}\,s^{-1}}$ following Laurent et al. (2010). Across the continent and throughout the year, the seasonal total of dust emission within the cyclone-affected area (Sect. 2.2) is most frequently less than $1\,\mathrm{g\,m^{-2}}$. Single regions and seasons, however, show distinct maxima of dust emission of up to $10\,\mathrm{g\,m^{-2}}$ that lie north of 20° N. Between December and February, peak emissions in the vicinity of the Atlas and Hoggar Mountains as well as in Libya are 2–$4\,\mathrm{g\,m^{-2}}$ (Fig. 9a). The areas where at least three intense emission events per season occur lie mostly away from the areas with the largest total emission. This points at moderate but frequent dust emissions in winter hot spots, while rather small total emissions in some regions are generated by a few intense events.

Spring shows larger dust emission of 4–$10\,\mathrm{g\,m^{-2}}$ associated to cyclones over a wider area (Fig. 9b). It is this season when the largest dust emission associated to cyclones occur. Peak emissions by cyclones are found south of the foothills of the Atlas Mountains, and as far east as the western fringes of the Libyan desert. Spring has more than

three intense emission events over most of the region north of 20° N. Areas with seasonal emission maxima have even larger numbers of intense emission events of more than six, partly more than nine events. This suggests that intense events substantially contribute to the largest emission amounts associated to springtime cyclones. It is
5   spring when the temperature contrast between land and sea is largest which favours the development of cyclones with high wind speeds.

The findings change dramatically in summer when maxima of the seasonal total dust emission associated to cyclones are situated over West Sahara and western parts of Mauritania with up to $6\,\mathrm{g\,m^{-2}}$ (Fig. 9c). More than six intense emission events are lim-
10 ited to the West African coast and coincide well with the largest seasonally total of dust emission. Here, surface signatures of AEWs may be deepest and cause the highest wind speeds (e.g. Thorncroft and Hodges, 2000). The coastal effect may be a contributing factor for strong winds in this region. In autumn, the number of intense emissions is here smaller with three events (Fig. 9d). It is this season when the seasonal total of
15 dust emission associated to cyclones is smallest over most of North Africa with less than $1\,\mathrm{g\,m^{-2}}$.

The fraction of the dust emission associated to migrating and long-lived cyclones relative to the total amount emitted per year is 4 % annually and spatially averaged over dust sources. Figure 10 shows the distribution of the fractional contributions of
20 cyclones annually averaged. Single regions in the northeast of Africa have contributions to dust emission by cyclones exceeding 10 %. The seasonal mean fraction of dust emission associated to cyclones is regionally larger in single seasons which are shown in Fig. 11. From December to February, substantial dust emission fractions associated to cyclones occur in areas north of 20° N only (Fig. 11a), because of the
25 limitation of cyclone tracks to northern locations (Fig. 4a). Here, the largest dust emission amounts associated to cyclones reach typical values of 5–15 % and lie between 15° W and 15° E. The dominant cyclone track over the eastern Mediterranean Sea in winter does not cause the majority of dust emissions in North Africa indicated by dust emission fractions below 5 % in regions east of 15° E. In spring, however, larger dust

Title Page

Abstract	Introduction
Conclusions	References
Tables	Figures

|◄ | ►|

◄ | ►

Back | Close

Full Screen / Esc

Printer-friendly Version

Interactive Discussion

emissions of 10–25 % are associated to cyclones in this region (Fig. 11b) when the main cyclone track shifts southwards onto the continent (Fig. 4b). This is the overall largest area and magnitude of cyclone contribution to dust emission in North Africa. Smaller areas with similar fractions of dust emission associated to migrating cyclones in spring lie to the south of the Atlas Mountains, to the northeast of the Hoggar Massif and in the Tibesti Mountains.

The dust emission associated to cyclones between June and August is shown in Fig. 11c. Contributions from regions north of 20° N drop to values below 5 % while isolated areas in Mali and Mauritania have contributions of 5–15 %. Typical contributions of cyclones to dust emission remain similar in autumn but the spatial pattern of hot spots changes (Fig. 11d). Higher values of around 15 %, now, occur in the centre of the Sahara, in the Western Great Erg and in the Libyan Desert (Fig. 11c and d). It is, however, important to underline that the dust emission flux connected to cyclones in the south is relatively small with seasonal totals below $1\,\mathrm{g\,m^{-2}}$. This implies that, even though the relative contribution is comparable to the north in winter and spring, the importance in terms of total dust mass is smaller (Fig. 9d).

In light of the large fractional contribution from depressions to dust emission (Sect. 3.4), the overall fractional contribution of migrating cyclones is surprisingly small. Springtime contributions of depressions of up to 90 % in the lee of the High Atlas change to contributions below 15 % when migrating cyclones are taken into account only (compare Fig. 8b and 11b). Over Libya, contributions from depressions are with values around 50 % also larger than the contribution from cyclones with maxima around 25 % during spring. Although a reduction is expected from the climatology with depressions to the one with cyclones, the magnitude of it is rather large particularly in the lee of the Atlas Mountains with a factor of six. The High Atlas is the region where the presence of lee troughs in the climatology of depressions is expected. These results indicate that only a few of these lee troughs develop to dust-emitting cyclones. Large and widespread dust emission associated to surface signatures of AEWs during summer do not occur as seen in the climatology of depressions. This result gives evidence

Dust emission by cyclones

S. Fiedler et al.

that most of the dust emitted during the presence of depressions is due to the Saharan heat low or other mechanisms embedded like NLLJs (Sect. 3.4).

Despite their small contributions to the total dust emission amount in the north, intense emission fluxes are regularly associated to migrating cyclones in spring (Fig. 11b). This aspect is analyzed further by defining a dust emission anomaly as the quotient of the dust emission associated to cyclones and the 20-yr mean of the dust emission flux in the same month. Figure 12 shows this anomaly factor along with the dust emission flux spatially averaged across dust-emitting grid boxes. The largest dust emission fluxes occur between February and May with values larger than $1.5 \times 10^{-6} \, \mathrm{g \, m^{-2} \, s^{-1}}$. It is this time of year when the largest total dust emission occur over the north (Fiedler et al., 2013). The anomaly factor during this season has values between four and eight, i.e. the dust emission associated to springtime cyclones is four to eight times larger than the long-term mean of the dust emission flux. The dust emission is smaller during summer with fluxes of $0.7–1.3 \times 10^{-6} \, \mathrm{g \, m^{-2} \, s^{-1}}$ while the anomaly factors increases to values of five to nine. Even larger anomaly factors are found between September and November with up to 20, but both the dust emission flux and the number of cyclones is then smallest. This result underlines that even though the total emission associated to migrating cyclones is rather small compared to the absolute emission in the north, the emission events during cyclone passage are particularly intense.

3.5.2 Dependency on cyclone quadrant

The areas of largest dust emission amounts associated to cyclones reside close to hot spots of cyclone tracks (Sect. 3.2). However, hot spots for cyclones and dust emission (Figs. 4 and 11) do not match perfectly due to two factors. On the one hand the location of peak winds within the cyclone-affected area is often away from the actual centre. On the other hand the parameterization of dust sources restricts the region of active emission within the cyclone-affected area. The map of potential dust sources enables dust emission in most areas of North Africa so that the location of peak winds is ex-

pected to be the dominant factor. The spatial distribution of the dust emission within the cyclone-affected area is investigated in the following. Since the emitted mass associated to cyclones is relatively small south of 20° N in general (Sect. 3.5.1), only the northern sub-domain is taken into account.

Figure 13 shows the annual cycle of the fraction of dust emission per quadrant of the cyclones north of 20° N spatially averaged. The results highlight that most dust is emitted in the northern quadrants with typical mean values of 30–55 % between November and March. In April, dust emission prevails in the northeast and southeast with about 30 % contribution each. Dust emission associated to cyclones in May is roughly equal distributed across the quadrants. June to September have clear maxima of dust emission in the southwest with 60–80 %. The total mass emitted between June and September, however, is smaller than at the beginning of the year (Fig. 9). Cyclones in October have most dust emission in the southeast, but the integrated mass of dust emission is smallest during autumn (Fig. 9d).

These result can be linked with the position of the highest wind speeds. In the case of a well-defined extra-tropical cyclone, the cool front typically lies to the west of the cyclone centre initially and moves towards the south and east thereafter. Peak winds, and therefore dust emission, are most likely at and behind the cool front as well as close to the cyclone centre due to the increased horizontal gradient of the geopotential height in these areas. Dust emission would primarily occur in the southwest initially, followed by prevailing emission in the southeast. At a later life stage, an extra-tropical cyclone typically forms an occlusion causing peak winds near the cyclone core. Dust emission may then form in all quadrants similarly. Integrated over the entire life time, most dust emission may be expected in southern quadrants if the cyclone has an extra-tropical character. While this is not found for the spatial average, examination of the spatial distribution of dust emission per quadrant (not shown) reveals that areas south of the Atlas Mountains show indeed more than 50 % of the dust emission in the southwest or southeast quadrants between February and May. This distribution complies with the expectation for extra-tropical cyclones. However, the lack of a southern maximum

Title Page

Abstract | Introduction

Conclusions | References

Tables | Figures

|◄ | ►|

◄ | ►

Back | Close

Full Screen / Esc

Printer-friendly Version

Interactive Discussion

in the spatial mean in winter and spring suggests that cyclones do not show typical characteristics of extra-tropical cyclones everywhere. Evaluating the spatial distribution of the dust emission per quadrant shows that dust emission in northern quadrants primarily occur in the central Sahara during spring. Here, the heat low lies typically to the south and relatively higher pressure northwards. This implies that instead of a classical frontal structure, a large horizontal gradient in the geopotential height occurs at the northern side of a large fraction of cyclones.

Summertime dust emission is mainly situated in the southwest of the cyclone centre in the spatial mean. Over West Africa, even larger emission fractions of up to 90 % occur in the southwest (not shown). The majority of cyclones during this season live particularly long and migrate westwards (Fig. 6a and c) pointing at surface signatures of AEWs. The dominant quadrant during this time of year is well in agreement with the position of emission ahead of AEWs where NLLJs are expected (Knippertz and Todd, 2010). The automated detection algorithm from Fiedler et al. (2013) is used for estimating the mean fraction of dust emission within the cyclone-affected area that coincide with the occurrence of NLLJs. The result suggests peak contributions from NLLJs to the dust emission associated to cyclones of 10–30 % over parts in West Africa (not shown). Another important driver for dust emission in association with AEWs are haboobs typically developing to the east of an AEW (Knippertz and Todd, 2010). The missing physical parameterization of these cold pools, as an important mechanism for dust emission during this time of the year and region (Heinold et al., 2013), may cause an underestimation of the dust emission to the east of AEWs. The diurnal cycle of dust emission indicates driving mechanisms on a sub-daily scale that is analyzed next.

3.5.3 Differences per time of day

Figure 14a shows the annual cycle of the total dust emission per time of day within the cyclone-affected area north of 20° N. Cyclones deflate a substantial amount of mineral dust in late winter and spring. Maxima occur during mid-day with peaks of 90–110 g m^{-2} in March, and 70–90 g m^{-2} in May in contrast to values below 20 g m^{-2}

between June and January (Fig. 14a). The dust emission during the influence of cyclones has a diurnal cycle with a distinct maximum during the daytime. Emission at night has typical values around $10\,\mathrm{g\,m^{-2}}$ and never exceeds $30\,\mathrm{g\,m^{-2}}$ during spring (Fig. 14a). At 09:00 UTC dust emission is often twice as large with maximum values of $60\,\mathrm{g\,m^{-2}}$ in May. Emissions at 12:00 and 15:00 UTC are even larger by a factor of two to four.

The diurnal differences can be explained by the development of the boundary layer. Dust emission occurs when the momentum transport to the surface is sufficiently large to exceed the threshold for emission onset. The stabilizing effect of surface cooling at night leads to a decrease of vertical momentum transfer to the surface. In contrast to the night, reduced stability during the day enables a larger transport of momentum to the Earth surface. It is this momentum transport that increases the near surface wind speed and mobilizes dust particles. The downward mixing of momentum is expected to be largest, when the daytime boundary layer is sufficiently deep for reaching a layer where high wind speed prevails, typically the free troposphere. Winter and spring is characterized by a relatively strong baroclinic zone at which the cyclone forms. The thermal wind describing the change of geostrophic wind over height is stronger the deeper (shallower) the warm (cool) air mass. The North African air mass is particularly deep compared to the air polewards due to the strong heating of the continent. The thermal wind is thus relatively large implying a strong increase of the geostrophic wind with height in the lower troposphere. Along with typically deep daytime boundary layers over North Africa momentum from the free troposphere is efficiently transported towards the surface. In the Sahara, the boundary layer reaches its largest depth at or closely after mid-day (Culf, 1992), that coincides well with the mid-day peak of dust emissions shown here. The time of maximum dust emission is in agreement with the observation of suspended dust in cyclones shown in Fig. 1.

The emission flux at 09:00 UTC in May, however, is almost as large as the mid-day values pointing at embedded NLLJs as a driving mechanism. The top of Fig. 14a shows the fraction of dust emission within the cyclone-affected area that is associated to

NLLJs. The latter are defined and automatically identified as in Fiedler et al. (2013). Based on these results, dust-emitting NLLJs are not frequently embedded in the cyclone-affected area with less than 10 % in winter and spring. This finding is well in agreement with the generally small dust emission amount associated to NLLJs during winter and spring in the north (Fiedler et al., 2013). The larger dust emission flux from cyclones at 09:00 UTC in May is, therefore, not linked to NLLJs. It seems most plausible that the momentum from the free troposphere is more efficiently mixed downwards in May than earlier in spring and winter. This is likely caused by a larger and earlier onset of the solar irradiation in late spring aiding the development of the daytime boundary layer.

NLLJs that can be embedded in AEWs are linked to 20 % of the dust emission in the cyclone-affected area in June and around 10 % in July and August. However, the total dust emission of summer is relatively small compared to spring. Haboobs may be the key driver in West Africa during summer (Heinold et al., 2013). AEWs are typically accompanied by deep moist convection the cold downdrafts of which may form an haboob (e.g. Knippertz and Todd, 2010). Haboobs are poorly represented in the 10 m-wind field of ERA-Interim (Marsham et al., 2011). Another reason for overall small dust emissions from AEWs may be the soil moisture effect that is discussed in the following section.

3.5.4 Impact of soil moisture

The dust emission amount associated to cyclones is smaller than the contribution estimated for depressions by one order of magnitude. One reason may be the weakening or suppressing effect of soil moisture on dust emission. While arid conditions prevail in North Africa, cyclones can produce rainfall. The magnitude of the effect is studied with a dust emission calculation without accounting for moisture (Sect. 2.2).

Figure 14b shows the annual cycle of the fraction of dust emission suppressed by the presence of soil moisture along with the total dust emission when moisture is taken into account as a benchmark. During late winter and spring, the time when dust emission

Title Page

Abstract | Introduction

Conclusions | References

Tables | Figures

◄ | ►

◄ | ►

Back | Close

Full Screen / Esc

Printer-friendly Version

Interactive Discussion

associated to cyclones show a clear maximum of 250–380 g m^{-2}, soil moisture suppresses roughly 10 % of the dust emission spatially averaged across the north. Other months show values ranging from 5 % to 20 %, but the total dust emission is smaller than 100 g m^{-2} in July and smaller than 80 g m^{-2} during the rest of the year. It is interesting that the value for the emission reduction by soil moisture during cyclone passage for the 20-yr period is of the same order of magnitude as the soil moisture effect for haboobs in August 2006 (Heinold et al., 2013). The spatial distribution of the fraction of dust emission associated to cyclones from Sect. 3.5.1 is robust against excluding the soil moisture in the dust emission calculation.

4 Conclusions

The present work provides the first climatological estimate of the amount of dust emission associated to depressions and cyclones over North Africa for 1989–2008. Dust emission simulations with the model by Tegen et al. (2002) driven by ERA-Interim forecasts show large dust emissions north of 20° N for December to May (Fiedler et al., 2013). Atmospheric depressions are tracked following the method from Schepanski and Knippertz (2011) for estimating the amount of dust emission associated to both depressions and migrating, long-lived cyclones. Depressions are abundant over North Africa due to the frequent formation of lee troughs and heat lows with maxima in the track density of up to 100 events. Cyclones migrating and living longer than 48 h, however, are less frequent with a total of 196 cyclones across North Africa. The cyclone track density compared to depressions is smaller by a factor ten. The smaller number of cyclones suggests that only few depressions, e.g. in the lee of the Atlas Mountains during spring, become migrating and long-lived cyclones.

The cyclone climatology highlights that 37 % of cyclones affecting North Africa occur in spring. Their centres most frequently lie north of 20° N with a clear cyclone track stretching from south of the Atlas Mountains towards the Eastern Mediterranean. This spatial pattern of the track density is in agreement with previous studies (Alpert et al.,

Springtime cyclones predominantly migrate eastwards, and live for three to seven days. The year-to-year variability of cyclones is largest during this season.

The depression and cyclone tracks are applied to the dust emissions for 1989–2008 in order to estimate their relative contribution to the dust emission amount. The results highlight that depressions coincide with 55 % of the dust emission while migrating and long-lived cyclones are associated with 4 % of the dust emission annually and spatially averaged for North African dust sources. Regionally larger contributions from both depressions and cyclones are found that vary with the season. The largest contributions from cyclones to dust emission are found during spring over wide areas in Libya with typically 15–25 %. The seasonal total of dust emission associated to cyclones is, here, amongst the largest with regionally 4–10 g m^{-2}. This dust emission amount associated to cyclones is up to one order of magnitude smaller than the seasonal mean dust emission for spring of regionally 10–50 g m^{-2} over Libya (Fiedler et al., 2013). Similar dust emission amounts associated to cyclones and fractional contributions to the seasonal total emission are found in isolated areas south of the Atlas Mountains. In contrast to cyclones, depressions show here contributions to dust emission with up to 90 % of the seasonal emission. These results suggest that the few migrating and long-lived cyclones do not emit the majority of dust aerosol in the north. However, the analysis of the emission flux magnitude reveals that emission events associated to cyclones are particularly intense. The dust emission flux during cyclone passage is larger than the climatological mean by a factor of four to eight. Another interesting aspect is that the dust emission associated to springtime cyclones is substantially larger during mid-day than at night by a factor of three to five. This result suggests that the growth of the boundary layer into the baroclinic zone of the cyclone is important for generating peak winds that are strong enough for mobilizing mineral dust. The effect of soil moisture on dust emission within the cyclone-affected area is a weakening on the order of 10 %.

In summer, AEWs play a role for dust emission in West Africa. It has been suggested that AEWs amplify here sufficiently for forming a signature close to the surface (Thorn-

Discussion Paper | Discussion Paper | Discussion Paper | Discussion Paper |

ACPD

13, 32483–32528, 2013

Dust emission by cyclones

S. Fiedler et al.

Title Page

Abstract   Introduction

Conclusions   References

Tables   Figures

◄   ►

◄   ►

Back   Close

Full Screen / Esc

Printer-friendly Version

Interactive Discussion

croft and Hodges, 2000). The results of the present study indicate that maximum contributions of AEWs to dust emission are 5–15 % but these are limited to isolated areas. The majority of the emissions within the cyclone-affected area is found in the southwestern quadrant of the AEW signature, i.e. the sector ahead of AEWs with northerly winds and potential NLLJ formation (Knippertz and Todd, 2010). NLLJs, defined as in Fiedler et al. (2013), coincide with 10–20 % of the monthly emissions associated to cyclones during summer while there are less than 10 % during the rest of the year. Larger dust emissions at the eastern side of AEWs are expected when haboobs are represented that are currently not parameterized but relevant for dust emission applications (Heinold et al., 2013). Contrary to AEWs, summertime depressions, like the Saharan heat low, coincide with up to 90 % of the dust emission across wide areas of North Africa. NLLJs form along the margins of the Saharan heat low (Fiedler et al., 2013) that are at least in parts included in the summertime dust emission associated to depressions.

In conclusion, the influence of depressions is important for dust emission across North Africa throughout the year. Migrating cyclones with life times of more than two days are comparably rare and do not substantially contribute to the total dust emission mass in most regions. However, cyclones generate intense dust emission fluxes making them nevertheless important for dust emission modelling. Large parts of the climatological dust emission maximum between November and May north of 20° N shown in Fiedler et al. (2013) are not associated to depressions and cyclones investigated here. Harmattan surges developing in consequence of post cold frontal ridging are proposed as another mechanism capable of emitting large amounts of dust aerosol. This dust storm type will be subject of future work.

Dust emission by cyclones

S. Fiedler et al.

Title Page

Abstract	Introduction
Conclusions	References
Tables	Figures

Back | Close

Full Screen / Esc

Printer-friendly Version

Interactive Discussion

References

Alpert, P. and Ziv, B.: The Sharav cyclone: observations and some theoretical considerations, J. Geophys. Res., 94, 18495–18514, 1989. 32486, 32487, 32491

Alpert, P., Neeman, B. U., and Shayel, Y.: Climatological analysis of Mediterranean cyclones using ECMWF data, Tellus A, 42, 65, doi:10.1034/j.1600-0870.1990.00007.x, 1990. 32486, 32487, 32496, 32497, 32507

Bou Karam, D., Flamant, C., Cuesta, J., Pelon, J., and Williams, E.: Dust emission and transport associated with a Saharan depression: February 2007 case, J. Geophys. Res.-Atmos., 115, D00H27, doi:10.1029/2009JD012390, 2010. 32486, 32487, 32491, 32493

Burpee, R. W.: The origin and structure of Easterly Waves in the lower troposphere of North Africa, J. Atmos. Sci., 29, 77–90, 1972. 32488, 32489, 32498

Carslaw, K. S., Boucher, O., Spracklen, D. V., Mann, G. W., Rae, J. G. L., Woodward, S., and Kulmala, M.: A review of natural aerosol interactions and feedbacks within the Earth system, Atmos. Chem. Phys., 10, 1701–1737, doi:10.5194/acp-10-1701-2010, 2010. 32485

Cornelis, W. M. and Gabriels, D.: The effect of surface moisture on the entrainment of dune sand by wind: an evaluation of selected models, Sedimentology, 50, 771–790, doi:10.1046/j.1365-3091.2003.00577.x, 2003. 32489

Culf, A. D.: An application of simple models to Sahelian convective boundary-layer growth, Bound.-Lay. Meteorol., 58, 1–18, doi:10.1007/BF00120748, 1992. 32505

Decker, M., Brunke, M. A., Wang, Z., Sakaguchi, K., Zeng, X., and Bosilovich, M. G.: Evaluation of the reanalysis products from GFSC, NCEP and ECMWF using flux tower observations, J. Climate, 25, 1916–1944, 2012. 32492

Dee, D. P., Uppala, S. M., Simmons, A. J., Berrisford, P., Poli, P., Kobayashi, S., Andrae, U., Balmaseda, M. A., Balsamo, G., Bauer, P., Bechtold, P., Beljaars, A. C. M., van de Berg, L., Bidlot, J., Bormann, N., Delsol, C., Dragani, R., Fuentes, M., Geer, A. J., Haimberger, L., Healy, S. B., Hersbach, H., Holma, E. V., Isaksen, L., Kallberg, P., Köhler, M., Matricardi, M., McNally, A. P., B. M. Monge-Sanz and, J.-J. M., Park, B.-K., Peubey, C., de Rosnay, P., Tavolato, C., Thepaut, J.-N., and Vitart, F.: The ERA-Interim reanalysis: configuration and performance of the data assimilation system, Q. J. Roy. Meteor. Soc., 137, 553–597, 2011. 32490, 32492

Fecan, F., Marticorena, B., and Bergametti, G.: Parameterization of the increase of the aeolian erosion threshold wind friction velocity due to soil moisture for arid and semi-arid areas, Ann.

Geophys., 17, 249–157, 1999, http://www.ann-geophys.net/17/249/1999/. 32489

Fiedler, S., Schepanski, K., Heinold, B., Knippertz, P., and Tegen, I.: Climatology of nocturnal low-level jets over North Africa and implications for modeling mineral dust emission, J. Geophys. Res.-Atmos., 118, 1–22, doi:10.1002/jgrd.50394, 2013. 32485, 32486, 32489, 32492, 32498, 32502, 32504, 32506, 32507, 32508, 32509, 32528

Hannachi, A., Awad, A., and Ammar, K.: Climatology and classification of Spring Saharan cyclone tracks, Clim. Dynam., 37, 473–491, doi:10.1007/s00382-010-0941-9, 2011. 32486, 32487, 32489, 32491, 32494, 32497, 32508

Heinold, B., Knippertz, P., Marsham, J. H., Fiedler, S., Dixon, N. S., Schepanski, K., Laurent, B., and Tegen, I.: The role of deep convection and nocturnal low-level jets for dust emission in summertimeWest Africa: estimates from convection-permitting simulations, J. Geophys. Res.-Atmos., 118, 1–16, doi:10.1002/jgrd.50402, 2013. 32485, 32489, 32498, 32504, 32506, 32507, 32509

Hodges, K. I., Lee, R. W., and Bengtsson, L.: A comparison of extratropical cyclones in recent reanalysis ERA-Interim, NASA MERRA, NCEP CFSR, and JRA-25, J. Climate, 24, 4888–4906, doi:10.1175/2011JCLI4097.1, 2011. 32487, 32494

Homar, V. and Stensrud, D. J.: Sensitivities of an intense Mediterranean cyclone: analysis and validation, Q. J. Roy. Meteor. Soc., 130, 2519–2540, doi:10.1256/qj.03.85, 2004. 32488

Homar, V., Ramis, C., and Alonso, S.: A deep cyclone of African origin over the Western Mediterranean: diagnosis and numerical simulation, Ann. Geophys., 20, 93–106, doi:10.5194/angeo-20-93-2002, 2002. 32488

Homar, V., Jansà, A., Campins, J., Genovés, A., and Ramis, C.: Towards a systematic climatology of sensitivities of Mediterranean high impact weather: a contribution based on intense cyclones, Nat. Hazards Earth Syst. Sci., 7, 445–454, doi:10.5194/nhess-7-445-2007, 2007. 32488

Hopsch, S. B., Thorncroft, C. D., Hodges, K., and Aiyyer, A.: West African storm tracks and their relationship to Atlantic tropical cyclones, J. Climate, 20, 2468–2483, doi:10.1175/JCLI4139.1, 2007. 32489

Huneeus, N., Schulz, M., Balkanski, Y., Griesfeller, J., Prospero, J., Kinne, S., Bauer, S., Boucher, O., Chin, M., Dentener, F., Diehl, T., Easter, R., Fillmore, D., Ghan, S., Ginoux, P., Grini, A., Horowitz, L., Koch, D., Krol, M. C., Landing, W., Liu, X., Mahowald, N., Miller, R., Morcrette, J.-J., Myhre, G., Penner, J., Perlwitz, J., Stier, P., Takemura, T., and Zender, C. S.:

Dust emission by cyclones

S. Fiedler et al.

Title Page

Abstract	Introduction
Conclusions	References
Tables	Figures

◀◀　　　▶▶

◀　　　▶

Back　　　Close

Full Screen / Esc

Printer-friendly Version

Interactive Discussion

Global dust model intercomparison in AeroCom phase I, Atmos. Chem. Phys., 11, 7781–7816, doi:10.5194/acp-11-7781-2011, 2011. 32485

Jones, C., Mahowald, N., and Luo, C.: The role of easterly waves on African desert dust transport, J. Climate, 16, 3617–3628, 2003. 32489

Kahana, R., Ziv, B., Enzel, Y., and Dayan, U.: Synoptic climatology of major floods in the Negev Desert, Israel, Int. J. Climatol., 22, 867–882, doi:10.1002/joc.766, 2002. 32487

Klose, M., Shao, Y., Karremann, M. K., and Fink, A.: Sahel dust zone and synoptic background, Geophys. Res. Lett., 37, L09802, doi:10.1029/2010GL042816, 2010. 32486

Knippertz, P. and Fink, A. H.: Synoptic and dynamic aspects of an extreme springtime Saharan dust outbreak., Q. J. Roy. Meteor. Soc., 132, 1153–1177, 2006. 32486, 32487, 32493

Knippertz, P. and Todd, M.: The central west Saharan dust hot spot and its relation to African easterly waves and extratropical disturbances, J. Geophys. Res.-Atmos., 115, D12117, doi:10.1029/2009JD012819, 2010. 32488, 32489, 32491, 32504, 32506, 32509

Knippertz, P. and Todd, M. C.: Mineral dust aerosols over the Sahara: Meteorological controls on emission and transport and implications for modeling, Rev. Geophys., 50, RG1007, doi:10.1029/2011RG000362, 2012. 32485

Laurent, B., Tegen, I., Heinold, B., Schepanski, K., Weinzierl, B., and Esselborn, M.: A model study of Saharan dust emission and distributions during the SAMUM-1 campaign, J. Geophys. Res., 115, D21210, doi:10.1029/2009JD012995, 2010. 32499, 32523

Lavaysse, C., Flamant, C., Janicot, S., Parker, D. J., Lafore, J.-P., Sultan, B., and Pelon, J.: Seasonal evolution of the West African heat low: a climatological perspective, Clim. Dynam., 33, 313–330, 2009. 32488, 32494, 32495

Luo, C., Mahowald, N., and Jones, C.: Temporal variability of dust mobilization and concentration in source regions, J. Geophys. Res., 109, D20202, doi:10.1029/2004JD004861, 2004. 32489, 32495

Maheras, P., Flocas, H., Patrikas, I., and Anagnostopoulou, C.: A 40 year objective climatology of surface cyclones in the Mediterranean region: spatial and temporal distribution, Int. J. Climatol., 21, 109–130, doi:10.1002/joc.599, 2001. 32486, 32487, 32490, 32494, 32508

Marsham, J., Knippertz, P., Dickson, N., Parker, D. J., and Lister, G.: The importance of the representation of deep convection for modeled dust-generating winds over West Africa during summer, Geophys. Res. Lett., 38, L16803, doi:10.1029/2011GL048368, 2011. 32485, 32489, 32506

Marticorena, B. and Bergametti, G.: Modelling the atmospheric dust cycle, 1: Design of a soilderived dust emission scheme, J. Geophys. Res., 100, 16415–16430, 1995. 32485, 32492

Mekonnen, A., Thorncroft, C. D., and Aiyyer, A. R.: Analysis of convection and its association with African easterly waves, J. Climate, 19, 5404–5421, 2006. 32488, 32489, 32497

Moulin, C., Lambert, C. E., Dayan, U., Masson, V., Ramonet, M., Bousquet, P., Legrand, M., Balkanski, Y. J., Guelle, W., Marticorena, B., Bergametti, G., and Dulac, F.: Satellite climatology of African dust transport in the Mediterranean atmosphere, J. Geophys. Res, 103, 13137–13144, 1998. 32487

Pedgley, D.: Desert depression over northeast Africa, Meteorol. Mag., 101, 228–244, 1972. 32496

Schepanski, K. and Knippertz, P.: Soudano-Saharan depressions and their importance for precipitation and dust: a new perspective on a classical synoptic concept, Q. J. Roy. Meteor. Soc., 137, 1431–1445, doi:10.1002/qj.850, 2011. 32486, 32487, 32488, 32490, 32491, 32507

Schepanski, K., Tegen, I., Laurent, B., Heinold, B., and Macke, A.: A new Saharan dust source activation frequency map derived from MSG-SEVIRI IR-channels, Geophys. Res. Lett., 34, L18803, doi:10.1029/2007GL030168, 2007. 32492, 32493, 32515

Schepanski, K., Tegen, I., Todd, M., Heinold, B., Bönisch, G., Laurent, B., and Macke, A.: Meteorological processes forcing Saharan dust emission inferred from MSG-SEVERI observations of subdaily dust source activation and numerical models, J. Geophys. Res., 114, D10201, doi:10.1029/2008JD010325, 2009. 32485, 32486, 32489, 32492, 32493

Shao, Y., Wyrwoll, K.-H., Chappell, A., Huang, J., Lin, Z., McTrainsh, G. H., Mikami, M., Tanaka, T. Y., Wang, X., and Yoon, S.: Dust cycle: an emerging core theme in Earth system science, Aerolian Res., 2, 181–204, 2011. 32485

Tegen, I., Harrison, S., Kohfeld, K., Prentice, I., Coe, M., and Heimann, M.: Impact of vegetation and preferential source areas on global dust aerosols: results from a model study, J. Geophys. Res., 107, 4576, doi:10.1029/2001JD000963, 2002. 32485, 32492, 32507

Thorncroft, C. D. and Hodges, K.: African easterly wave variability and its relationship to Atlantic tropical cyclone activity, J. Climate, 14, 1166–1179, 2000. 32488, 32489, 32495, 32497, 32498, 32500, 32508

Thorncroft, C. D., Hall, N. M. J., and Kiladis, G. N.: Three-dimensional structure and dynamics of African easterly waves, Part III: Genesis, J. Atmos. Sci., 65, 3596–3607, doi:10.1175/2008JAS2575.1, 2008. 32488

Todd, M., Allen, C., Bart, M., Bechir, M., Bentefouet, J., Brooks, B., Cavazos-Guerra, C., Clovis, T., Deyane, S., Dieh, M., Engelstaedter, S., Flamant, C., Garcia-Carreras, L., Gandega, A., Gascoyne, M., Hobby, M., Kocha, C., Lavaysse, C., Marsham, J., Martins, J., McQuaid, J., Ngamini, J. B., Parker, D., Podvin, T., Rocha-Lima, A., Traore, S., Wang, Y., and Washington, R.: Meteorological and dust aerosol conditions over the Western Saharan region observed at Fennec supersite-2 during the Intensive Observation Period in June 2011, J. Geophys. Res.-Atmos., 118, 8426–8447, doi:10.1002/jgrd.50470, 2013. 32488

Trigo, I. F., Davies, T. D., and Bigg, G. R.: Objective climatology of cyclones in the Mediterranean region, J. Climate, 12, 1685–1696, 1999. 32486, 32487, 32494, 32508

Trigo, I. F., Bigg, G. R., and Davies, T. D.: Climatology of cyclogenesis mechanisms in the Mediterranean, Mon. Weather Rev., 130, 549–569, 2002. 32486, 32487

Wernli, H. and Schwierz, C.: Surface cyclones in the ERA-40 dataset (1958–2001), Part I: Novel identification method and global climatology, J. Atmos. Sci., 63, 2486–2507, doi:10.1175/JAS3766.1, 2006. 32490

Winstanley, D.: Sharav, Weather, 27, 146–160, doi:10.1002/j.1477-8696.1972.tb04279.x, 1972. 32486, 32487, 32489

a) 20-02-2013, 12 UTC b) 09-03-2013, 15 UTC c) 05-04-2011, 15 UTC
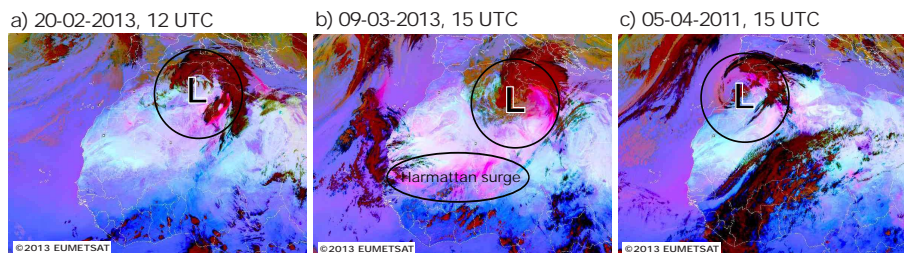
Fig. 1. Observations of cyclones and associated dust aerosol over North Africa. Shown here are false-colour images from MSG-SEVIRI (e.g. Schepanski et al., 2007) indicating mineral dust aerosol (pink) and clouds (red and black). Circles and ellipse mark the cyclone-affected area with a radius of 10° and dust emission associated to a Harmattan surge, respectively.
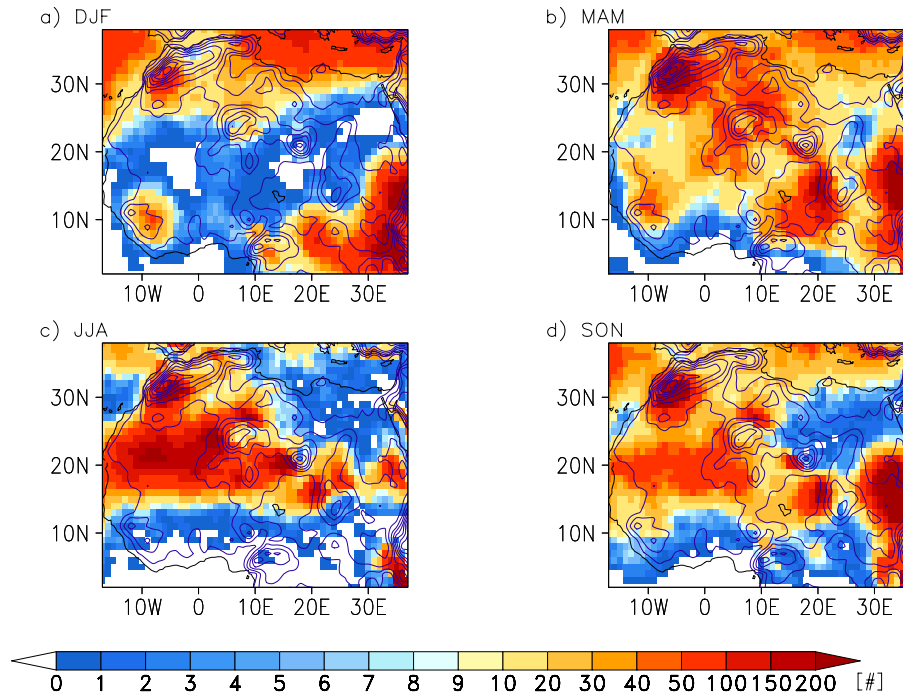
Fig. 2. Track density of all identified depressions. Climatology of total depression number for **(a)** December–February, **(b)** March–May, **(c)** June–August, and **(d)** September–November for 1989–2008 based on the depression centre defined by the outermost closed contour in the geopotential height at 925 hPa from the tracking algorithm (Sect. 2.1). Contours show orography in steps of 200 m.
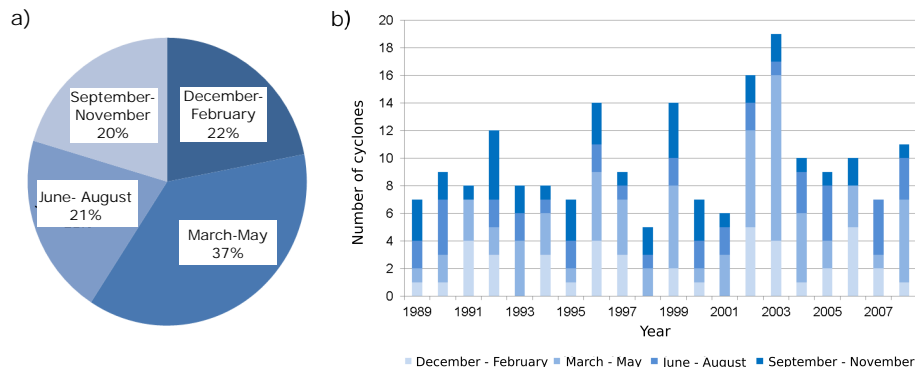
Fig. 3. Seasonal and interannual variations of long-lived and migrating cyclones. **(a)** Seasonal distribution of cyclones and **(b)** time series of cyclones in the sub-domain 0°–40° N and 20° W–45° E for 1989–2008.
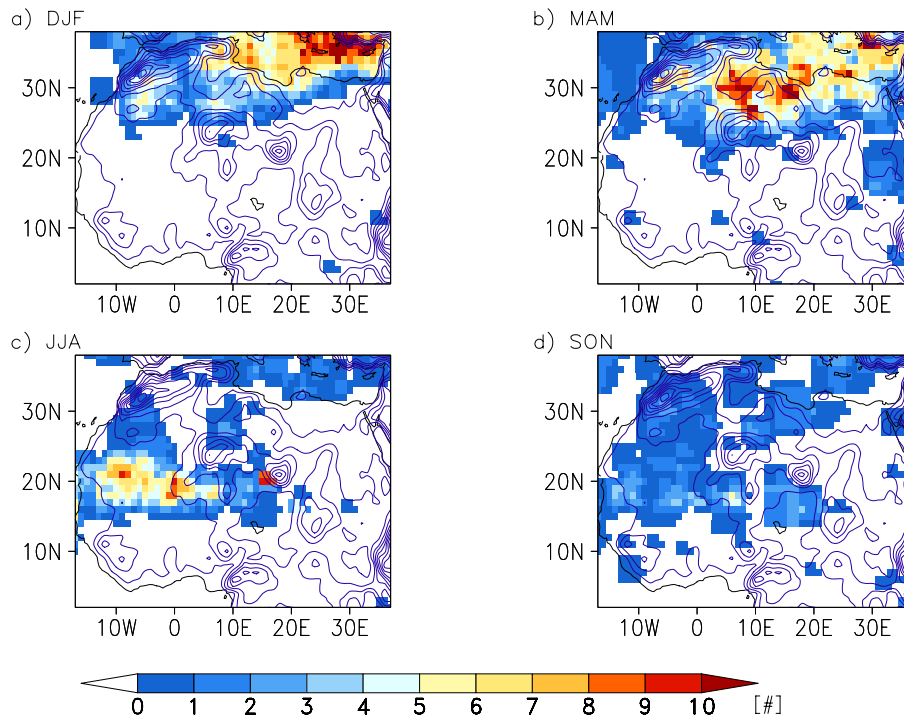
Fig. 4. Track density of long-lived and migrating cyclones. Climatology of total cyclone number for **(a)** December–February, **(b)** March–May, **(c)** June–August, and **(d)** September–November for 1989–2008 based on the cyclone centre defined by the outermost closed contour in the geopotential height at 925 hPa from the tracking algorithm (Sect. 2.1). Contours show orography in steps of 200 m.
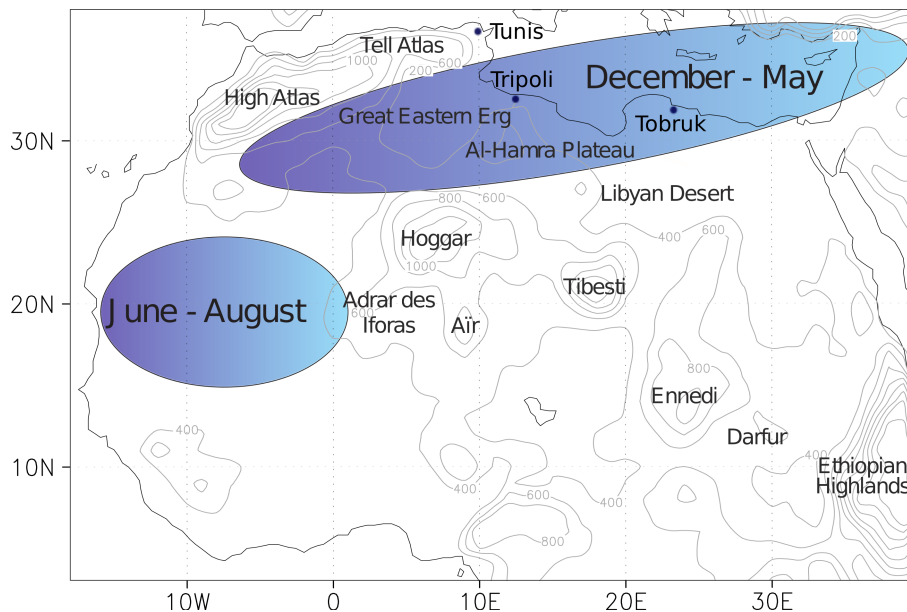
Fig. 5. Schematic overview on regions of most frequent cyclone occurrence. Contours show orography in steps of 200 m based on ERA-Interim. Geographical terms used in the text are indicated.

Full Screen / Esc

Printer-friendly Version

Interactive Discussion
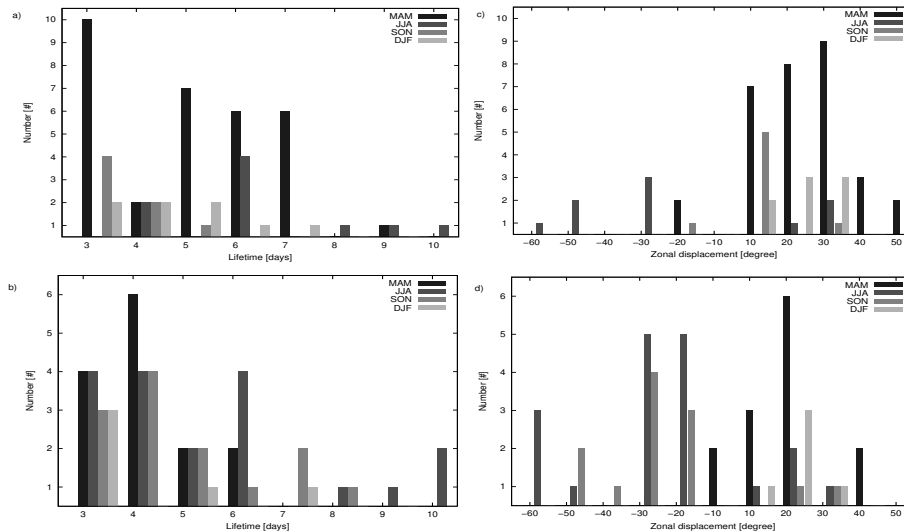
Fig. 6. Histograms of characteristics from long-lived and migrating cyclones. Cyclone life times for 1989–2008 forming **(a)** in the north (15° W–35° E, 20° N–32° N), and **(b)** in the south (15° W–35° E, 0° N–20° N); and zonal displacement of cyclone centres during their life time forming **(c)** in the north, and **(d)** in the south.
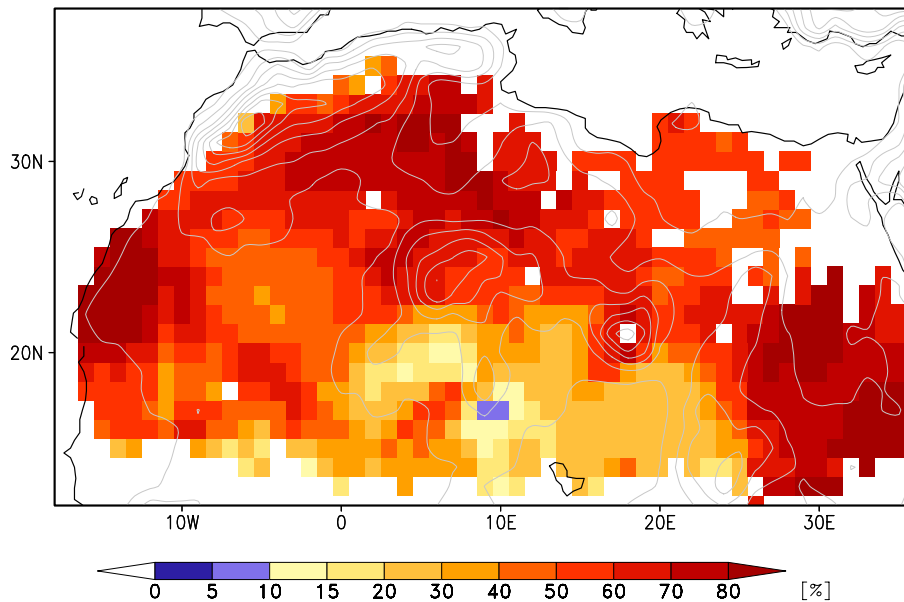
Fig. 7. Annual fraction of dust emission amount associated to depressions. Shown is the contribution to the total dust emission in percent averaged for 1989–2008. Contours show orography in steps of 200 m.
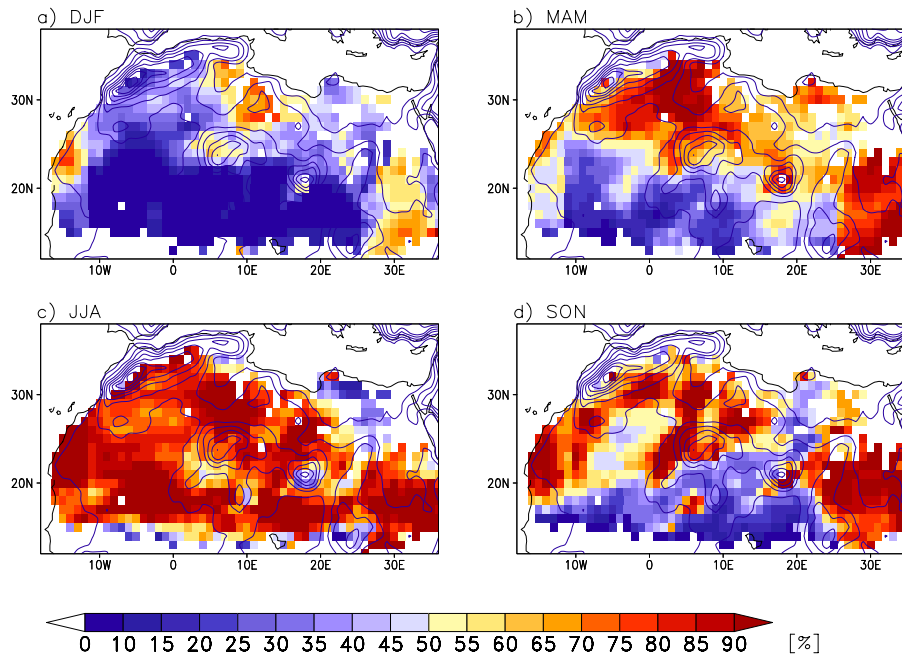
Fig. 8. Seasonal fraction of dust emission amount associated to depressions. Shown are contributions in percent for **(a)** December–February, **(b)** March–May, **(c)** June–August, and **(d)** September–November averaged for 1989–2008. Contours show orography in steps of 200 m.
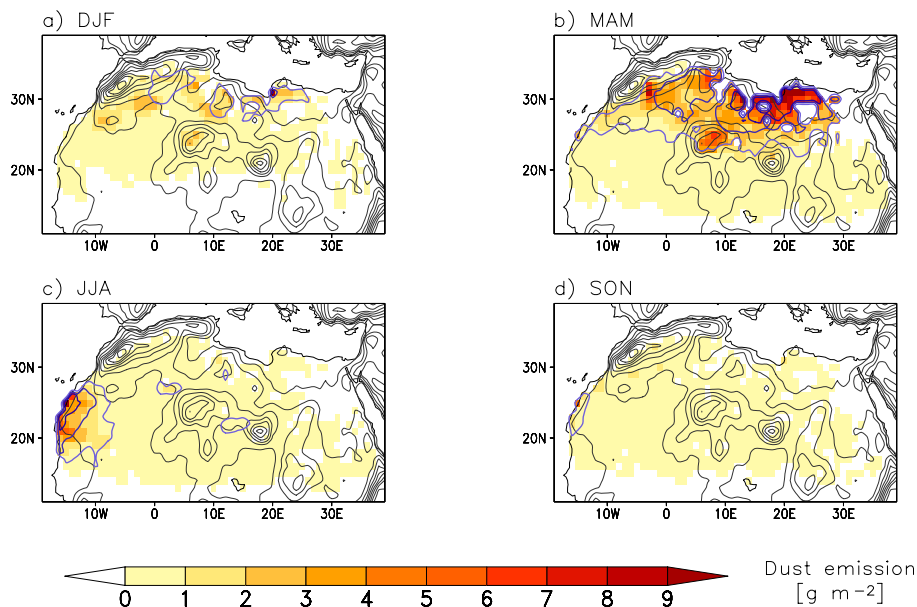
Fig. 9. Seasonal dust emission associated to long-lived and migrating cyclones. Shown are mean emissions (shaded) for **(a)** December–February, **(b)** March–May, **(c)** June–August, and **(d)** September–November averaged for 1989–2008. Black contours show orographic height in steps of 200 m. Blue contours show the number of intense dust emission events, defined by a flux larger than $10^{-5}\,\mathrm{g\,m^{-2}\,s^{-1}}$ following Laurent et al. (2010), in steps of three events.

Fig. 10. Annual fraction of dust emission amount associated to long-lived and migrating cyclones. Shown is the contribution to the total dust emission in percent averaged for 1989–2008. Contours show orography in steps of 200 m.

Fig. 11. Seasonal fraction of dust emission amount associated to long-lived and migrating cyclones. Shown is the contribution to the total dust emission in percent for **(a)** December–February, **(b)** March–May, **(c)** June–August, and **(d)** September–November averaged for 1989–2008. Contours show orography in steps of 200 m.
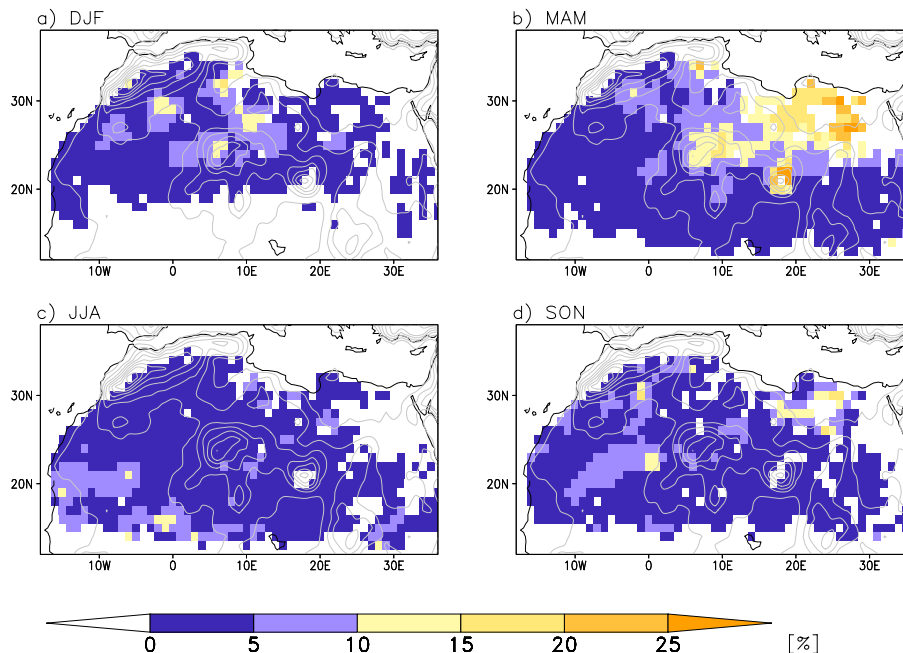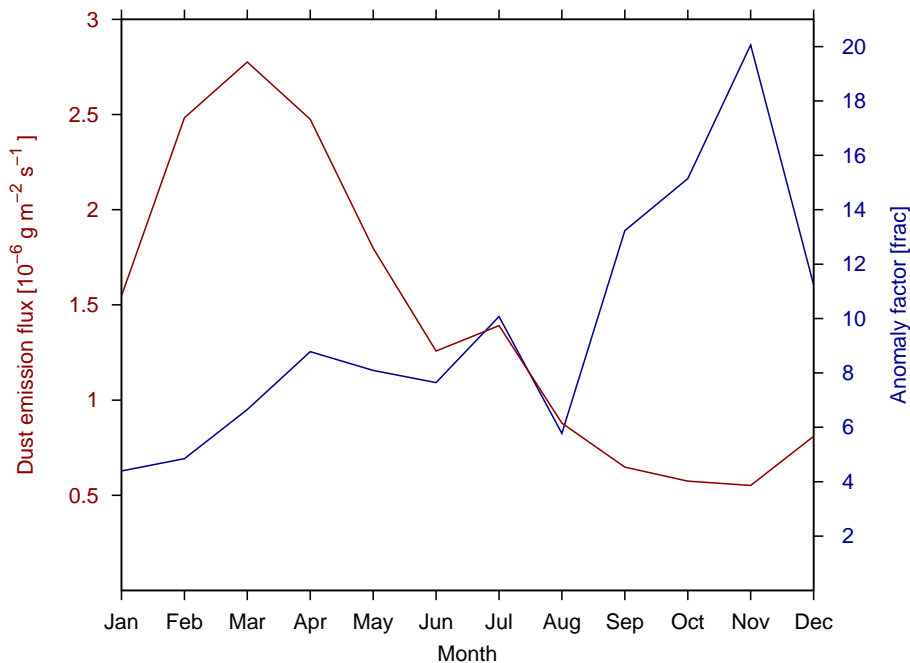
Full Screen / Esc

Printer-friendly Version

Interactive Discussion

Fig. 12. Intensity of dust emission fluxes associated to long-lived and migrating cyclones. Annual cycle of the dust emission flux (red) and the intensity of the dust emission associated to cyclones shown as anomaly factor (blue) averaged over dust-emitting grid boxes for 1989–2008. The anomaly factor is defined as the quotient of the dust emission flux associated to the cyclone and the 20-yr mean of the dust emission flux of the same month.

Fig. 13. Monthly fraction of dust emission from the four quadrants of long-lived and migrating cyclones averaged for the northern sub-domain (15° W–40° E and 20° N–40° N) and for 1989–2008.

Title Page

Abstract | Introduction

Conclusions | References

Tables | Figures

|◄ | ►|

◄ | ►
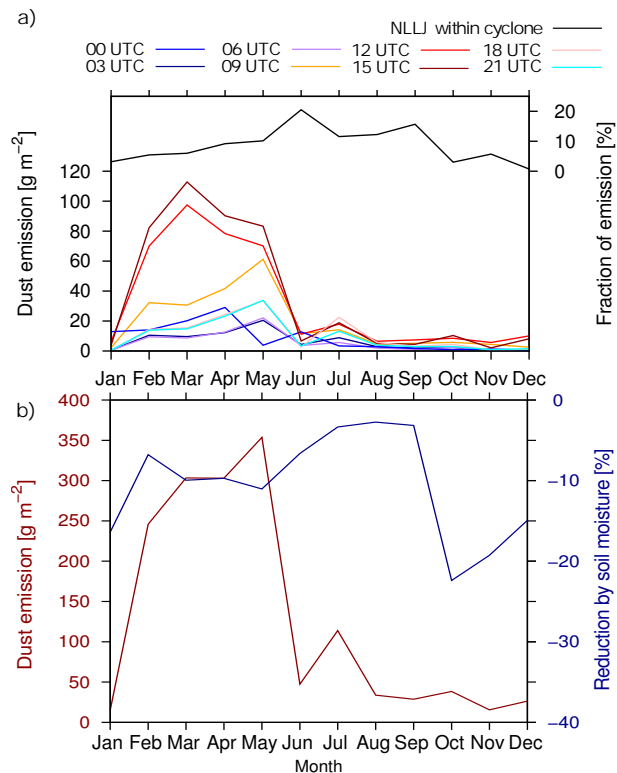
Back | Close

Full Screen / Esc

Printer-friendly Version

Interactive Discussion

Fig. 14. Total dust emission amount associated to long-lived and migrating cyclones. Annual cycle **(a)** of dust emission for different times of the day (colour) and of the fraction of dust emission associated with cyclones coinciding with NLLJ events; **(b)** of the total dust emission and of the fraction of dust emission suppressed by soil moisture. Values are spatially integrated over the northern sub-domain (15° W–40° E and 20° N–40° N) and monthly averaged over 1989–2008. NLLJ events are identified as in Fiedler et al. (2013).

Title Page

Abstract | Introduction

Conclusions | References

Tables | Figures

|◀ | ▶|

◀ | ▶

Back | Close

Full Screen / Esc

Printer-friendly Version

Interactive Discussion